Tunneling and dispersion in 3D phononic crystals

John H. Page*,[I], Suxia Yang[I, II, 1], Zhengyou Liu[III], Michael L. Cowan[I, 2], Che Ting Chan[II] and Ping Sheng[II]

[I] Department of Physics and Astronomy, University of Manitoba, Winnipeg, Manitoba R3T 2N2, Canada
[II] Department of Physics, Hong Kong University of Science and Technology, Clear Water Bay, Kowloon, Hong Kong, China
[III] Department of Physics, Wuhan University, Wuhan 430072, China

Received November 9, 2004; accepted January 21, 2005

Phononic crystal / Ultrasound / Acoustic band gaps / Tunneling of ultrasound / Group velocity dispersion

Abstract. Tunneling and dispersion of ultrasonic pulses are investigated in 3D phononic crystals consisting of 0.8 mm-diameter tungsten carbide beads that are close packed in a *fcc* crystal array embedded in either water or epoxy. Pulsed ultrasonic techniques allow us to measure the phase velocity and group velocity, i.e. the dynamics of wave propagation, as well as the transmission coefficient. Our experimental data are well interpreted using multiple scattering theory (MST). In the tungsten carbide/water crystals, dispersion phenomena were studied at frequencies in and around the gap in the ΓL direction. A strong suppression of the group velocity, and large variations of the group velocity dispersion (GVD) were found at frequencies around the band edges. By contrast, fast group velocities and nearly constant GVD with values around zero were observed at gap frequencies, indicating that tunneling in phononic crystals is essentially dispersionless. In the tungsten carbide/epoxy crystals a wide gap (*to our knowledge, largest measured 3D band gap*) was measured covering a frequency range from 1.2 MHz to 4.3 MHz along the ΓL crystal direction. The agreement between the theory and experiments gives strong evidence for the existence of a large complete gap (1.5 MHz to 3.9 MHz), which is theoretically predicted from the band structure calculations.

1. Introduction

During the past two decades, increasing attention has been drawn to two new types of artificial material, photonic crystals and phononic crystals. Phononic and photonic crystals are periodic elastic or dielectric composites with lattice constants comparable to the wavelength of sound or light [1–50]. In other words, they are acoustic (ultrasonic or sonic) and electromagnetic (optical or microwave) analogues of atomic crystals. Due to the periodicity of these crystals, there can be frequency ranges where wave propagation is forbidden, giving rise to spectral gaps, which are analogous to electronic band gaps. Because photonic and phononic crystals are similar in many ways, we first outline some of the essential developments related to the photonic crystals, before focusing on phononic crystals.

Much of the initial interest in photonic crystals revolved around the question of whether *complete* photonic band gaps, i.e., frequency ranges where optical modes are forbidden along all crystal directions, could be realized, and if they could, what interesting properties would result [1, 2]. For example, a perfect photonic crystal would provide perfect dielectric mirrors at the gap frequencies. Introduction of point defects and/or line defects in a perfect photonic crystal would trap the light around and/or along the defects, with potential applications as micro-cavities and/or wave guides. Thus photonic crystals provide a way of blocking, trapping and channeling light. Many theoretical investigations have shown that the appearance of complete gaps requires the optimization of many parameters, such as the refractive index contrast, lattice type, filling fraction and "atom" configurations [4–12]. Experimentally, photonic crystals have been constructed with different dimensions at different frequency ranges, although the fabrication of high quality 3D photonic crystals with band gaps in the visible regime remains a challenge. Another way of "channeling" light was proposed more recently by employing the super-prism and super-lens effects, where the propagation of light is sensitive to the frequency and incident angle of the incident beam [14, 15]. This method is based on the anisotropy of the equifrequency surfaces and complete band structures are not required. One example of a potential application of these effects is in wavelength-division multiplexed (WDM) communication for telecommunications or data links. In terms of basic physics, localization [16–18] and wave dynamics [19–22] for waves at the frequencies in and around band gaps has also been explored. It was found that a single photon or wave pulse could tunnel through a finite slab of the crystals at gap frequencies [19–21], while at the band edges, a strong reduction of the group velocity and large dispersion effects were observed [22].

* Correspondence author (e-mail: jhpage@cc.umanitoba.ca)
[1] Current address: Dept. of Materials Science & Engineering, University of Toronto, Toronto, ON, Canada M5S 3E4
[2] Current address: Department of Physics, University of Toronto, Toronto, ON Canada M5S 3E3

Elastic (or acoustic) wave propagation in phononic crystals has also gained much attention recently because of the rich physics that arises from the additional physical parameters that enter the problem. These include the density contrast and Lamé constants, as well as the existence of longitudinal wave modes and their mixture with transverse waves [23–50]. Potential applications of phononic crystals, e.g., in noise-proof devices and sound filters, have also attracted much interest [38, 40]. Compared with the extensive exploration of photonic crystals, the study of phononic crystals has a shorter history, during which much of the attention has been mainly focused on the existence of complete phononic band gaps.

Underpinning many of the phononic crystal research efforts are theoretical predictions/simulations of phononic band structures. The plane-wave (PW) method [23–25], based on the expansion of the periodic coefficients (density, velocities) in the wave equation as Fourier sums, has been the most popular approach. Using this model, extensive band-structure calculations for acoustic or elastic waves propagating in 2D (rods in a host material) and 3D (scatterers in a homogenous matrix) periodic composites have been performed, where both the rods/scatterers and matrix are either fluids or solids. These calculations have shown how the existence of a phononic band gap depends not only on the crystal structure [52] but also on the density contrast, velocity differences, the volume fraction of one of the two components and their shapes. Among these parameters, density contrast plays the most important role. Although the PW model is very useful for predicting the properties of a variety of systems, it is found to have convergence problems in dealing with mixed crystals, such as solid scatterers in a liquid matrix, due to the vanishing shear modulus in the fluid component. Based on the KKR (Korringa, Kohn and Rostoker) approach for electrons, a multiple scattering theory (MST) for acoustic and elastic band gap materials has recently been developed [26–28]. MST yields more accurate results than the PW approach for systems with spherical scatterers and can handle the mixed crystals, e.g., solid scatterers in a liquid matrix. A layered MST [27, 28] was also developed, which calculates the transmission and reflection for a finite system, thus providing a direct comparison with the experiments. As will be seen later, the MST gives an excellent description for our phononic crystals.

Compared to the theoretical studies, there have been fewer experimental investigations of phononic crystals. Also many of the previous experiments have involved transmission measurements and 2D systems. The phase information, which is very important for delineating the wave dynamics and investigating the band structure, has been neglected in many of the experiments. In this paper, we systematically study ultrasonic wave transport through 3D phononic crystals, using pulsed ultrasound techniques for the experiments and the MST for the theoretical simulations. The pulsed ultrasonic techniques allow us to measure not only the frequency dependence of the transmission coefficients but also the phase velocity and group velocity. Hence a more complete picture of the wave dynamics is obtained. In previous papers, we reported ultrasound tunneling and focusing by negative refraction in 3D mixed crystals consisting of tungsten carbide beads in water [43, 49]. Here, we continue the study of the same mixed crystals, reviewing and extending our investigation of tunneling and presenting new data on anomalous dispersion in and around the first band gap. In addition to the mixed crystals, we discuss wave properties in solid crystals consisting of tungsten carbide or steel beads in epoxy, where the existence of remarkably large band gaps is demonstrated.

This paper is structured as follows. Section 2 describes the experimental measurements and the methods used to analyze the data. It is followed by a short description of the MST in Section 3. Results and discussion are given in Sections 4 and 5, where we compare theory with experiments and interpret our experimental data for the two crystal systems. Finally, we present some conclusions in Section 6.

2. Experiment

Two types of phononic crystals were constructed. The first is a "mixed" phononic crystal, with solid scatterers (tungsten carbide beads) immersed in a liquid matrix (water). The other is a solid crystal with tungsten carbide or steel beads embedded in epoxy. This choice of materials provides a large scattering contrast in our ultrasonic experiments, due to the large differences in both the density and velocity of the scatterers and the surrounding matrix materials (see Table 1).

For all the samples, the beads were assembled in a *fcc* crystal structure with the beads packed in triangular layers perpendicular to the body diagonal, or along the [111] direction. The beads are very monodisperse, with diameters of 0.800 mm (tungsten carbide) and 0.8014 mm (steel), which made it possible to make very high quality crystals. Templates were designed to ensure the beads were constrained in triangular layers that were arranged in an ABCABC... sequence. These templates had a flat hexagonal bottom with outward sloping sidewalls, such that the angle of inclination (with respect to the horizontal) of each adjacent wall alternated between 54.74° and 70.33°. By putting the beads in carefully by hand, we obtained very high quality crystals. The samples had 49 beads on each side of the bottom hexagonal layer, so that there were a large number of beads (more than 6000) in each layer. Thus the boundary reflections at the perimeter of each layer could be neglected. For a n-layer crystal, the thickness L of the crystal is $d[1 + (n-1)\sqrt{2/3}]$, where d is the diameter of the beads.

There were some differences in the templates for the two different sample systems. The template for the tungsten carbide/water sample was made of acrylite. The beads were placed horizontally on top of a substrate, which was made sufficiently thick (7.1 cm) that multiple reflections

Table 1. Properties of the component materials in our crystals.

Material	Density (kg/m^3)	Longitudinal velocity (km/s)	Shear Velocity (km/s)
Tungsten carbide	13.8	6.655	3.23
Steel	7.67	6.01	3.23
Water	1.0	1.49	0
Epoxy	1.1	2.6	1.5

of the ultrasonic pulse traveling in the substrate arrived too late to interfere with the signals that were transmitted through the crystals. However for the solid tungsten carbide/epoxy sample, a substrate was no longer needed to hold the beads in place after the epoxy cured, so that it was important to select a substrate material that allowed the solid crystal to be easily pealed off the template after it was made. Teflon was found to work well for this purpose. For each template, all the parts were made separately and were well polished to the required tolerances before being screwed together.

The tungsten carbide/water samples were always held horizontally in order to allow gravity to keep the beads in place in the template, and obviate the need for a top plate to prevent the beads from falling out. The ultrasonic waves transmitted through the sample were measured by placing the sample between two transducers and immersing the whole system in a large water tank, which provided an excellent coupling medium between the ultrasonic transducers and the sample. A $^1/_2$-inch-diameter planar immersion generating transducer was placed far away from the bottom of the sample and used to generate an input pulse that was a plane wave to a good approximation. The transmitted pulses were detected by a receiving transducer that was placed above the crystal. The detected pulses were amplified with a low-noise bandpass amplifier, averaged with a digital oscilloscope and then downloaded to a computer for further analysis. The input pulse was determined by measuring the pulse transmitted through the substrate alone, without the sample in place.

We assembled the solid crystals when the epoxy was in a liquid state. From the many possible types of epoxy available, we selected Maraglas 655, because it is hard, has relatively little ultrasonic absorption, and has a long working life, allowing the beads to be assembled in position before the viscosity became too large. On completion of the bead assembly process, the crystals, together with the template, were put in an oven at 60 °C for 48 hours to let the epoxy cure. The solid samples were then taken out from the template, and any excess epoxy was polished off. For the solid crystals, the sample was oriented vertically, and the sample signals were compared directly with reference pulses in water.

3. Theory

As mentioned in the Introduction, the PW theory fails to give an accurate description of mixed composites, such as solid scatterers in a liquid host. Based on Korringa-Kohn-Roskoker (KKR) theory for electronic band-structure calculations, we use a multiple scattering theory (MST) for elastic systems with spherical scatterers. By calculating the exact Mie scattering for a single scatterer and solving the resulting secular equation for the whole system, one can determine the band structure of the phononic crystal. Details of the calculation can be found in Liu *et al.* [28].

To get a direct comparison between the theory and experiments, we also developed a layer MST for a slab of crystal with a finite number of layers of beads. The key of this approach is the combination of the scattering matrix relating the input and scattered waves for two single-layer crystals to get the scattering matrix for a 2-layer crystal, as illustrated in Fig. 1. Repeating this procedure, the scattering matrix for a crystal with arbitrary number of layers can be obtained. For a multi-layer crystal with thickness L, the transmitted wave is given by

$$T(L,\omega) = A(L,\omega)\exp\left[i\varphi(L,\omega)\right], \tag{1}$$

where A is the transmitted amplitude normalized by the incident wave (*i.e.*, the transmission coefficient), and φ is the cumulative phase relative to the input wave. Besides the transmission coefficient, one can also determine the phase velocity and group velocity from Eq. (1), since

$$v_p = \omega L/\varphi\,; \qquad v_g = \mathrm{d}\omega/\mathrm{d}k = L\,\mathrm{d}\omega/\mathrm{d}\varphi\,. \tag{2}$$

In Figs. 2 and 3, we compare the MST predictions for the band structures of our crystals with the amplitude transmission coefficients for 7-layer thick samples along the [111] direction. For the mixed tungsten carbide/water crystals, a large complete band gap is seen, covering a frequency range from 0.98 MHz to 1.2 MHz [43], with the stop band along the [111] direction extending from 0.8 to 1.2 MHz. In the middle of the gap, the transmission for a 7-layer crystal drops by almost a factor of 100. By contrast, for the solid tungsten carbide/epoxy crystals, there is also a complete band gap, but it is *much* larger, extending from about 1.5 to 3.9 MHz, a frequency range that is 90% of the mid-gap frequency. As can be seen in Fig. 3, the position of the gap defined by the transmission calculation agrees fairly well with the band structure calculation. However, the position of upper band edge is a little higher for the transmission coefficient, a difference that results from the finite sample effect: theoretically the band structure calculation is based on an infinite crystal. Perhaps the most striking result shown by the transmission calculation for the solid crystal (right panel of Fig. 3) is the very small transmission that is predicted in the band gap: the

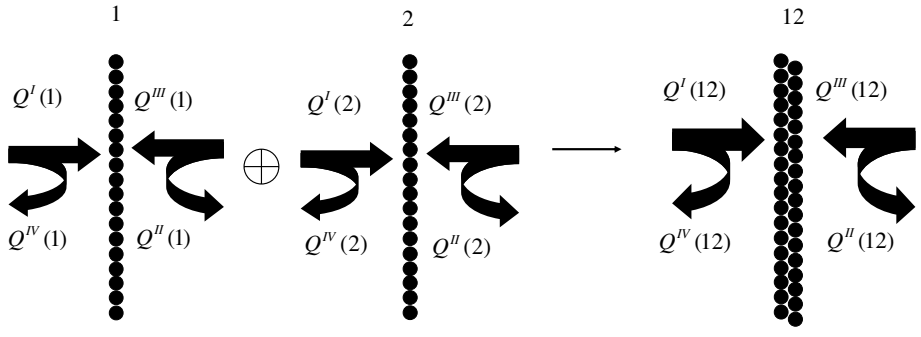

Fig. 1. Schematic graph showing how to calculate the scattering matrix for a 2 layer phononic crystal from that for two 1-layer crystals.

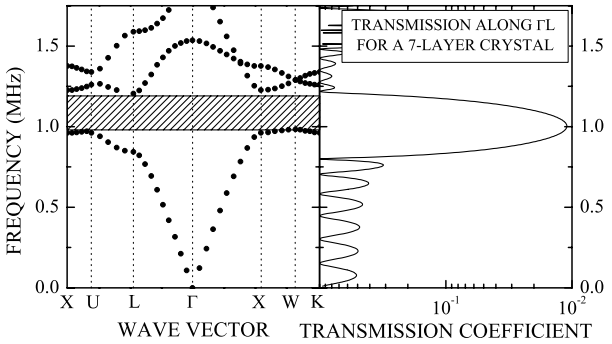

Fig. 2. Left panel: band structure of a *fcc* crystal consisting of tungsten carbide beads (diameter 0.8 mm) in water. Right panel: MST predictions for the frequency dependence of the amplitude transmission coefficient near the band gap for a 7-layer crystal.

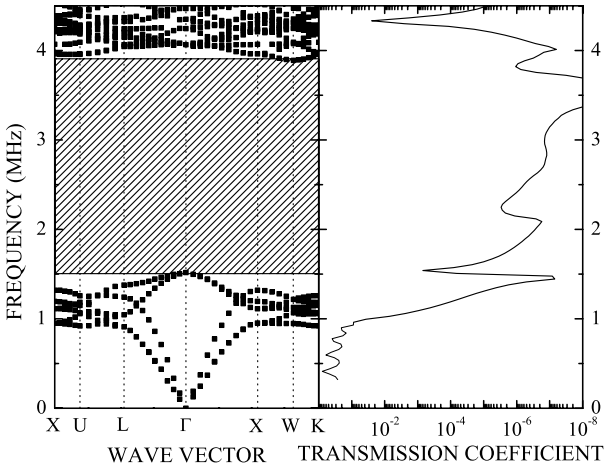

Fig. 3. Left panel: band structure of a *fcc* crystal consisting of tungsten carbide beads (diameter 0.8 mm) in epoxy. Right panel: MST predictions for the frequency dependence of the amplitude transmission coefficient for a 7-layer crystal.

amplitude transmission coefficient for a 7-layer crystal is reduced by 7 orders of magnitude compared to the maximum transmission in the pass band. Comparison between these theoretical predictions and experimental data is given in the next two sections.

4. Tungsten carbide/water crystals

Mixed crystals of tungsten carbide beads in water were chosen as an ideal system in which to study wave propagation near a band gap, since this combination of solid and liquid materials has one of the largest possible density differences between the scatterers and the matrix, and is sufficient to ensure a complete gap for the *fcc* structure [43–44, 49]. In this section, we review how ultrasonic experiments and multiple scattering theory can be used to gain an in-depth understanding of how band gaps dramatically affect the properties and character of waves in periodic media, and then focus on the large dispersion effects that we have observed in this system.

When a pulse is transmitted through a phononic crystal, both the amplitude and phase show large variations with frequency. By taking the ratio of the magnitudes of the Fourier transforms of the transmitted and input pulses, the frequency

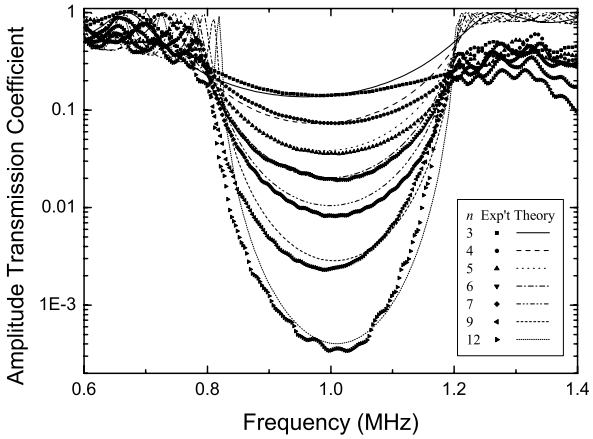

Fig. 4. Frequency dependence of the amplitude transmission coefficient along [111] near the band gap at 1 MHz for the tungsten carbide/water phononic crystals.

dependence of the amplitude transmission coefficient can be determined over the bandwidth of the transducers used. Results for a large number of sample thicknesses are shown in Fig. 4, where the experimental data are also compared with the predictions of the Multiple Scattering Theory. The large drop in the transmission near 1 MHz shows that the stop band in the [111] direction extends from approximately 0.8 to 1.2 MHz. This figure also shows that the amplitude A decreases exponentially with sample thickness in the band gap, consistent with a change from propagating modes outside the gap to evanescent modes inside the gap. These evanescent waves have an imaginary wave vector $\varkappa$ and decay as $A(L) = A_0 \exp[-\varkappa L]$, with $\varkappa = 0.93\ \mathrm{mm}^{-1}$ in the middle of the gap. The (complex) Fourier transforms of the transmitted and input pulses also allow the change in phase of the transmitted waves relative to the input waves (i.e. the phase difference) to be measured as a function of frequency. Results for a 6-layer and 12-layer tungsten carbide/water crystal are shown in Fig. 5a, where the experimental data (symbols) are compared with the predictions of multiple scattering theory (solid curves). As for the

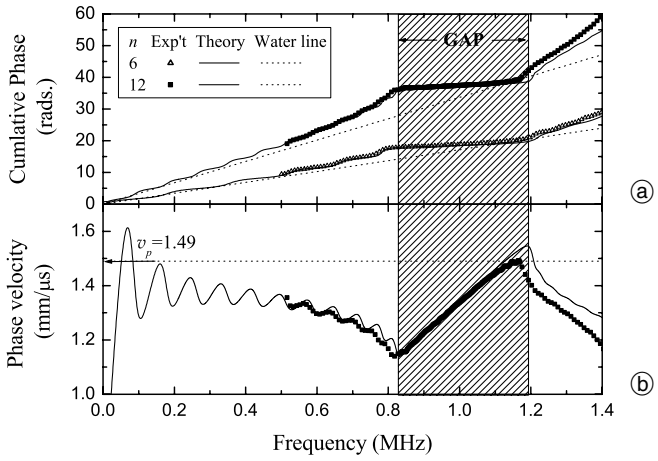

Fig. 5. (**a**) The frequency dependence of the cumulative phase along the [111] crystal direction for 6-layer and 12-layer tungsten carbide/water samples. The solid lines are the theoretical predictions from the MST and symbols are the experimental data. The guide lines (dotted lines) are the results for waves in pure water. (**b**) The frequency dependence of the phase velocity for the 12-layer sample.

transmission, good overall agreement between experiment and theory can be seen, although the experimental phase change above the band gap is somewhat larger, due to a small shift in the upper band edge. To compare with the wave properties in a homogenous material, the phase changes through the same distances in pure water are indicated by the dotted guide lines (these water lines play the same role here as light lines for photonic crystals). At low frequencies or in the long wavelength limit, waves cannot resolve each scatterer, as the wavelength of the sound is much bigger than the lattice constant. Thus the dispersion relationship should be linear at low frequencies, so that the phase change goes to 0 as frequency goes to 0. Hence the ambiguity of 2π in the inverse tangent function can be eliminated, and the true cumulative phase measured and calculated as a function of frequency over the entire frequency range. At the lowest frequencies, the phase change through the crystal is very close to that in water, but substantial differences appear as the frequency gets higher. In particular, at the frequencies inside the gap, the phase change through each crystal exhibits a plateau of magnitude $n\pi$, where n is the number of layers; this is a nice demonstration that the condition for Bragg scattering, namely that the layer thickness be equal to half the wavelength, is satisfied in the band gap. At higher frequencies, the cumulative phase continues to increase, showing that, unlike phonons in atomic crystals, phase changes greater than π per layer are directly measured and physically meaningful.

Figure 5b shows the frequency dependence of the phase velocity in the vicinity of the band gap, as determined directly from the cumulative phase using equation (2). At low frequencies, the phase velocity approaches the water velocity. Below the band gap, the phase velocity exhibits $n-1$ oscillations, where n is the number of layers, an interference effect resulting from boundary reflections that correspond to normal modes of the crystal; these oscillations are also seen in the transmission and the cumulative phase, but are more pronounced in the phase velocity. In the vicinity of the gap, a strong frequency dependence is seen, indicating that dispersive effects may be important in this range of frequencies. These are discussed in more detail below.

The measurements of cumulative phase also allow the dispersion curve, ω versus $k = \varphi/L$, to be measured directly in the extended zone scheme. The results along the [111] direction are shown in Fig. 6, where the experimental data are again compared with the MST. The large gap near 1 MHz is evident from the sharp rise in the dispersion curve, followed at higher frequencies by a more gradual increase. Interestingly, the narrow stop band near 1.5 MHz is barely discernable in the experimental data, although it does show up in the theoretical predictions, which lie above the experimental data between the gap and the 4th pass band. These data for the dispersion curve in the extended zone scheme can be folded back into the reduced zone scheme and compared with theoretical predictions for the band structure. Good agreement between experiment and theory is found, as shown in Ref. [43], which gives a good example of how ultrasonic measurements can be used to investigate the band structure of phononic crystals.

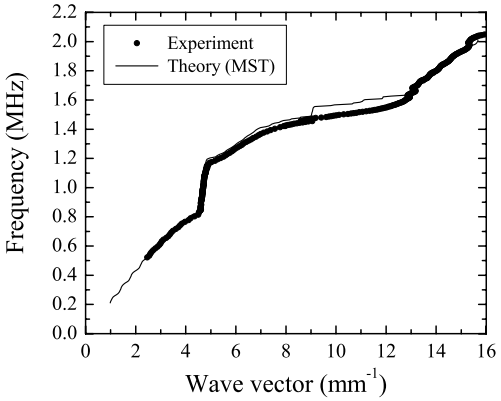

Fig. 6. Comparison of the measured dispersion curve along the ΓL direction in the extended zone scheme with the predictions of the layer MST.

The observation that the transmitted amplitude in the band gap decays exponentially with sample thickness suggests that tunneling may be involved. To investigate this possibility in more detail, and to gain additional insight into the character of the modes inside the band gap, we also measured the group velocity as a function of sample thickness [43, 44]. These experiments were performed by measuring the transit time of the peak of a narrow band Gaussian pulse through crystals that were 3 to 12 layers thick, using a digital filtering technique. Not only were large values of the group velocity measured at all thicknesses (in all cases significantly larger than the velocity in water), but the velocity was found to increase with thickness (see Fig. 7), an unusual result that is characteristic of tunneling in quantum mechanics [52]. However, the experimental values of v_g were smaller than the theoretical predictions of the MST when no absorption is present in the crystals, as can be seen by comparing the solid circles with the open squares in Fig. 7. This figure also shows that for thicknesses greater than 5 layers of beads, the MST predictions with no absorption are described accurately by L/t_g, with a constant value of the tunneling time $t_g = 0.54\ \mu s$ (solid line), as expected for tunneling when $\varkappa L \gg 1$. The reduction in the measured values of v_g rela-

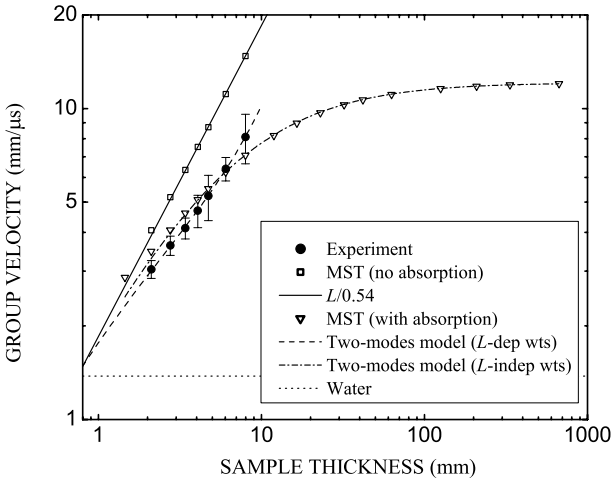

Fig. 7. Dependence of the group velocity on thickness for the tungsten carbide/water phononic crystals.

tive to these theoretical predictions can be explained by absorption in the phononic crystals, an effect that has a simple physical interpretation: In the band gap, the role of absorption is to make the destructive interference that gives rise to the band gap incomplete, with the result that a small amplitude propagating mode survives in addition to the evanescent tunneling mode. Quantitative agreement with the experimental results was obtained using the "two-modes" model, which assumes the two modes contribute to the measured group time in parallel, so that the group velocity can be calculated from the weighted average of the tunneling time t_{tun} and the propagation time $t_{\text{prop}} = L/v_{\text{prop}}$. Thus, $\bar{v}_g = L/[w_t t_{\text{tun}} + w_p(L/v_{\text{prop}})]$, where t_{tun} and v_{prop} are independent of thickness, and w_t and w_p are the weighting factors. These weighting factors are proportional to the coupling coefficients and attenuation factors of each mode i, $c_{\text{i}} \exp[-\varkappa_i L]$ [43, 44]. The best fit to the data, shown by the dashed curve in Fig. 7, was obtained with $c_{\text{tun}} = 0.95$, showing that the tunneling mode is dominant, and with an attenuation factor that is slightly larger for the propagating mode, suggesting that the propagating component becomes gradually less important as the thickness increases over this range. The excellent fit to the data shows that this simple model can successfully account for the effects of absorption on the tunneling of ultrasonic waves in phononic crystals, and provide a clear physical picture of the underlying physics.

These results also raise an interesting question: does absorption lead to a saturation of the group velocity in very thick samples, so that the transit time no longer becomes independent of sample thickness as in the "pure" tunneling case? To investigate this question, we have also calculated the group velocity by incorporating absorption into the MST by making the longitudinal modulus of the water complex. (Since the ultrasonic energy density inside the beads is less than 1% of the energy density in water at frequencies inside the band gap, absorption in the beads has little effect). These MST predictions, calculated using an absorption coefficient $\varkappa_{\text{abs}} = 0.072\ \text{mm}^{-1}$, are shown by the open triangles in Fig. 7 over a very large range of sample thicknesses, well beyond those at which the transmitted signal has become too small to measure experimentally. Thus, for this constant value of dissipation, the group velocity is predicted to become independent of thickness at sufficiently large thicknessess, reaching a value that is approximately 8 times the velocity in water; in other words, the tunneling time is predicted to be much shorter than for normal propagation in water, but increases with thickness in this large thickness limit. Again this behaviour can be fitted using the two modes model, providing the attenuation factors are identical for the tunneling and propagation modes so that the weighting factors are independent of thickness. The result of this fit is shown by the dot-dashed curve in Fig. 7, giving an excellent parameterization of the results of the MST calculation, and showing that the enhancement of the group velocity in the large thickness limit is a consequence of the relatively small weighting of the propagating component ($\sim$14% in this case). Note that, in the experimentally accessible range of thicknesses, the MST predicts a slower dependence on thickness than is observed experimentally, suggesting that the absorption actually decreases with thickness in our crystals. This decrease in absorption with thickness is not unreasonable, since one of the important contributions to dissipation is almost certainly frictional losses due to the relative motion of the beads as the ultrasonic wave passes through the crystal; these frictional losses are reduced in thick samples where the beads are more constrained by the weight of the beads in the layers above. As a result, in our experiments the increase in the group velocity with thickness is larger than predicted for constant absorption, and the characteristics of tunneling clearly dominate the observed behaviour of the group velocity. Thus, not only has the tunneling of ultrasound been convincingly demonstrated in these phononic crystals, but our experiments and theory have also allowed the rather unusual effects of dissipation on evanescent modes to be studied in some detail. This dissipation has no counterpart for tunneling of a particle in quantum mechanics.

The large variation in the frequency dependence of the cumulative phase near the band gap suggests other interesting questions: Is the tunneling of a pulse dispersive, and how significant is the dispersion near the band edges? In photonic crystals, large dispersive effects near the band edges have been found [22], but in these experiments the crystals were too thick to allow measurements inside the gap, because the transmission at gap frequencies was too small to detect. However, such effects have not been studied in phononic crystals, suggesting that a systematic study of dispersion in phononic crystals is warranted. To address this issue, we have investigated the frequency dependence of not only the wave vector k, but also the inverse group velocity and the group velocity dispersion (GVD). Here the inverse group velocity β_1 is defined by the first derivative of the wave vector k with respect to angular frequency ω, i.e., $\beta_1 = \mathrm{d}k/\mathrm{d}\omega$, and the group velocity dispersion β_2 is defined by its second derivative, i.e., $\beta_2 = \mathrm{d}^2k/\mathrm{d}\omega^2$. The results of these measurements for a 5-layer tungsten carbide/water phononic crystal are shown in Fig. 8.

As can be seen from Fig. 8, the wave vector (bottom panel) increases with frequency in the pass bands with some oscillations, just as does the cumulative phase

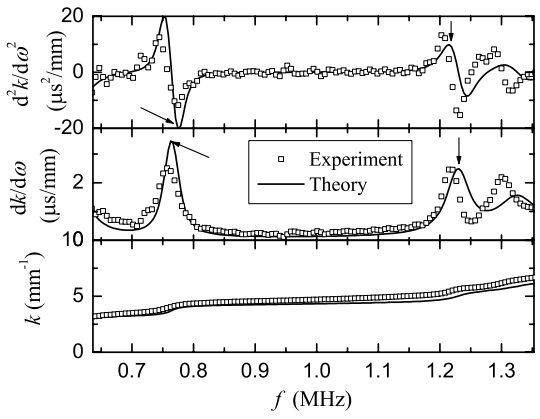

Fig. 8. Measured wave vector, inverse group velocity and group velocity dispersion (open squares) for a 5-layer tungsten carbide/water crystal as a function of frequency. Theoretical predictions are given by the solid lines.

shown in Fig. 5a. However inside the band gap, k is almost constant over a wide frequency range, exhibiting a very small, almost linear increase with frequency. This means that the first order derivative (inverse group velocity) should be very small, while the second order derivative (GVD) and all higher order derivatives should be nearly zero. This is clearly seen in data for β_1 and β_2 shown in top two panels of Fig. 8. In particular, the GVD, which determines the change in the width of a pulse as it propagates through a medium, is consistent with zero within experimental error. In other words, no measurable dispersion of a pulse inside the band gap is expected on the basis of these data, even though the scattering is very strong and the phase velocity varies considerably (Fig. 5b). This further demonstrates that the wave does not propagate in a normal way through a phononic crystal at the gap frequencies, and that tunneling is essentially dispersionless.

In contrast to the lack of dispersion at frequencies inside the gap, the inverse group velocity (middle panel of Fig. 8) shows peaks at the band edges, which means there is a strong suppression of the group velocity on both sides of the band gap. At the band edges, the group velocities are only about 0.4 mm/μs, much less than the normal sound velocity in either component (water: 1.49 mm/μs, tungsten carbide: longitudinal velocity 6.655 mm/μs and transverse velocity 3.23 mm/μs). The theory gives good overall agreement with the measurements, although there is a small shift in the experimental data relative to the theory at frequencies above the band gap, indicating that the measured gap width is slightly less than the predicted one.

From the behaviour of the group velocity dispersion shown in the top panel of Fig. 8, we can see that at the frequencies below the gap, the GVD increases rapidly, reaching a maximum positive value and then dropping quickly to a minimum negative value before approaching zero at the band gap. At frequencies above the gap, it behaves in the opposite way, having a maximum closest to the band edge, followed by a sharp minimum. This behaviour reflects the modal structure that is clearly resolved in thin samples, and masks the smooth increase in the GVD that is expected from the average curvature seen in the dispersion relation (Fig. 6) below the band gap, and the negative GVD that would be expected from the average curvature of the dispersion curve above the band gap. Thus, the way in which the GVD approaches zero at the band edges is different to the predictions for thick crystals in Ref. [22], where it is pointed out that the group velocity dispersion should rapidly decrease to zero from its maximum positive value below the gap and increase rapidly to zero from its minimum negative value above the gap.

Figure 9 gives some real examples of pulse envelopes to show explicitly how the dispersion affects the transmitted pulse shapes at different frequencies. This figure shows three long pulses (bandwidth 0.02 MHz) with central frequencies at the lower band edge (0.744 MHz), inside the band (0.972 MHz) and at the upper band edge (1.2 MHz), transmitted through the same 5-layer phononic crystal of tungsten carbide beads in water. Here, the centers of the input pulses are set to time zero. These input

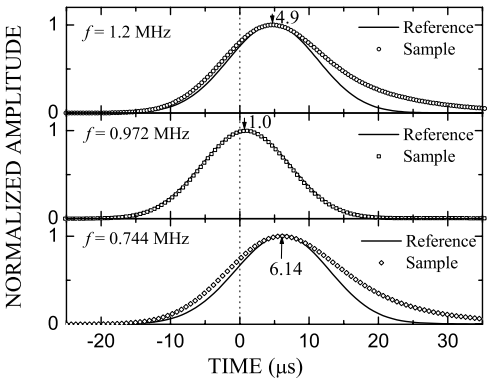

Fig. 9. A demonstration of pulse broadening at different frequencies (at the lower band edge, inside the band, and at the upper band edge). The pulse bandwidth is 0.02 MHz. The reference pulses (solid lines) have the same shape as the input pulses, which are centred at 0, but are manually shifted to a later time to make the comparison with sample pulses (open squares) clearer. Thus the positions of the peaks of the sample signals reflect how long it took for the input pulses to travel through the sample at a certain frequency.

pulses are not plotted for the purpose of clarity. In order to clearly show the distortion of the transmitted pulses, we normalize both the sample and input pulses to the same peak magnitude, and shifted the input pulses (solid lines) so that the peaks align with those of the sample pulses (open squares). Thus, the peak positions of the sample signals still reflect how long it took for the input pulses to travel through the sample, but the shapes of the transmitted and input pulses can readily be compared. It is worth noting that in all three cases, the peak pulse travel times accurately correspond to the group times calculated from the derivative of the phase with frequency, via the definition of the group velocity as $v_g = \mathrm{d}\omega/\mathrm{d}k$.

It can be seen that, at the frequency inside the gap, it takes much less time for the pulse to travel (tunnel [43]) through the sample and that no distortion of the pulse occurs, consistent with the prediction of the GVD measurements that tunelling is dispersionless. By contrast, the pulses at frequencies near both band edges travel much slower and in both cases there is significant pulse broadening. However, since the band width is very narrow, only about 2.7% of the smallest central frequency, the transmitted pulses are still fairly symmetric and the group velocity can still be defined and accurately measured.

To end this section, we examine how the inverse group velocity and group velocity dispersion evolve as the crystal thickness is varied, both at gap frequencies and at frequencies near the band edges. The theoretical predictions and experimental data are given in Figs. 10 and 11, respectively. We first present the theoretical results (Fig. 10). In the top panel, we plot the thickness dependence of the (negative) GVD ($\mathrm{d}^2k/\mathrm{d}\omega^2$) at the first dip at the lower band edge (solid squares), the positive GVD (solid triangles) at the first peak at the upper band edge (as indicated by arrows in Fig. 8), and the GVD in the middle of the gap at 0.947 MHz (open circles). It can be seen that the GVD in the gap is independent of the sample thickness with a value near zero. This is consistent with the prediction given by Imhof *et al.* for photonic crystals [22]. However, the magnitude of the GVD increases with sample

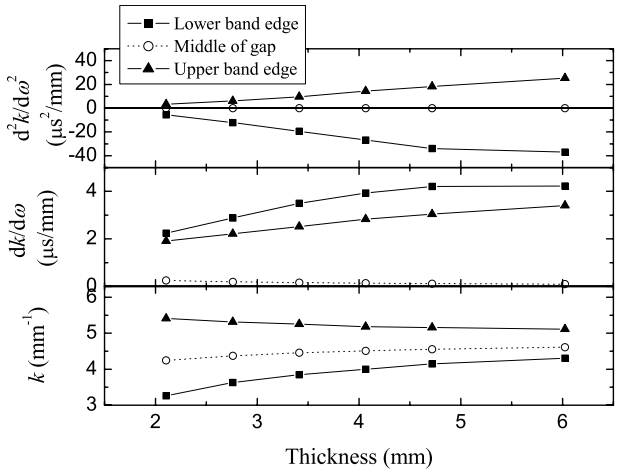

Fig. 10. Theoretical predictions from MST for the thickness dependence of the wave vector and its first and second derivatives with respect to frequency at the lower band edge, the middle of the gap and the upper band edge.

thickness at frequencies around both band edges. The two peak values of the inverse group velocity for both band edges (solid squares/triangles for lower/upper band edges respectively) and at a frequency of 0.947 MHz (open circles) are plotted in the middle panel, and the corresponding wave vectors are given in the bottom panel. It can be seen that the inverse group velocities at the gap frequency are very small and decrease with thickness, which means fast group velocities characteristic of tunneling. However, the inverse group velocities at frequencies around the band edges are very large and increase with the sample thickness, which means a large suppression of the group velocity. The values of the wave vector at the upper and lower inverse group velocity maxima (lower panel) move closer together, reflecting a narrowing of the band gap as the thickness increases. The experimental data (Fig. 11) show the same trends, but both the inverse group velocity and GVD have smaller values than the theoretical predictions due to absorption, which was not accounted for in these calculations.

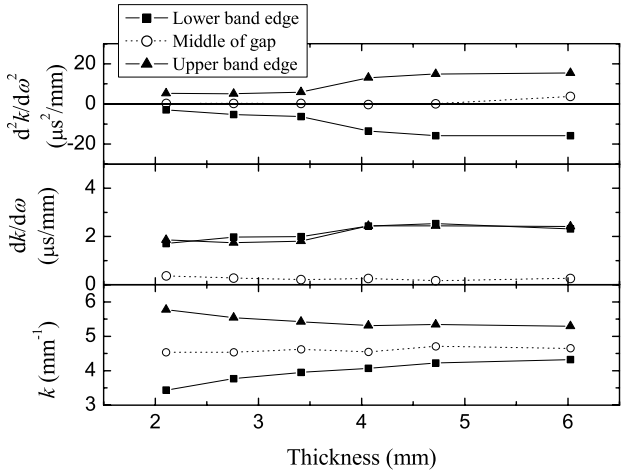

Fig. 11. Measured thickness dependence of the wave vector and its first and second derivatives with respect to frequency at the lower band edge, the middle of the gap and the upper band edge.

5. Tungsten carbide/epoxy crystals

To demonstrate experimentally the conditions under which very large phononic band gaps can be realized in three-dimensional phononic crystals, we have also studied solid 3D crystals consisting of tungsten carbide or steel beads in epoxy. Our MST calculations for the tungsten carbide/epoxy system (Fig. 3) predict a very wide band gap for this system, a result that is consistent with previous calculations for other combinations of solid scatterers in a solid matrix [23, 45]. Thus, this type of phononic crystal appears to be ideal for achieving wide gaps, but to our knowledge no experiments have yet been reported on such three dimensional systems. Because they are structurally more robust than the mixed crystals considered in the previous section, solid crystals may also be better suited for developing potential applications, such as ultrasound filters, sound mirrors, and other novel ultrasound devices.

The large increase in gap width that results from replacing a liquid matrix by a solid one is shown in Fig. 12, where we compare the measured transmission coefficient for two 4-layer phononic crystals consisting of tungsten carbide or steel beads in epoxy. These data also demonstrate the effect of density contrast on the gap width. To facilitate comparison with the mixed crystals, the transmission coefficient was again measured along the [111] direction. It can be seen that the band gaps are very wide for both samples. These data appear to be the first to show that such wide and deep gaps can actually be observed experimentally. The band gap of the steel/epoxy sample extends in frequency from 1.3 MHz to 3.7 MHz, while the gap of the tungsten carbide/epoxy sample is wider, covering frequencies from 1.2 MHz to 4.3 MHz. Also the gap for tungsten carbide/epoxy sample is about 10 times deeper than that of the steel/epoxy sample. The diameter of the steel beads is 0.8014 mm, very close to tungsten carbide beads (0.800 mm diameter), and the crystal structures and orientations are the same for two crystals. Thus the difference of the gap width can only be attributed to the

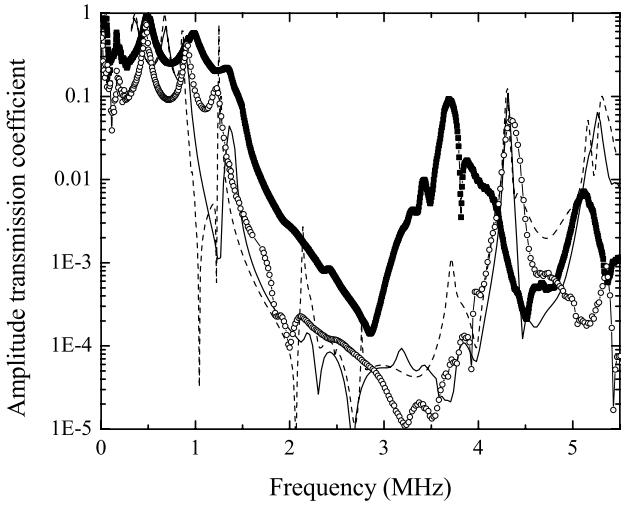

Fig. 12. Measured amplitude transmission coefficients as a function of frequency for 4-layer crystals of steel beads in epoxy (solid symbols) and tungsten carbide beads in epoxy (open symbols). The dashed and solid curves are the predictions of the MST without and with absorption respectively.

difference in elastic properties of steel and tungsten carbide (Table 1). As the sound velocities are almost the same for steel and tungsten carbide, the difference is almost entirely due to the density difference alone. Thus, in addition to showing that very large gaps can be achieved, our measurements provide an experimental proof of the theoretically predicted effect of the density contrast on the gap width [23–24].

As can also be seen from Fig. 12, the waves are strongly attenuated in the band gap; for the tungsten carbide crystal, the amplitude drops by 4 orders of magnitude for a crystal that has only 4 layers (2.76 mm thick). Also shown are the theoretical MST predictions for the tungsten carbide/epoxy crystal. Since ultrasonic absorption is greater in epoxy than in water at these frequencies, it is important to account for the effects of absorption in the epoxy matrix. This was done by using complex Lamé constants for epoxy, based on measurements of the absorption coefficient in pure epoxy near 2.5 MHz, which lies in the middle of the relevant frequency range. The solid curve (MST with absorption) and dashed curve (MST without absorption) in Fig. 12 show that absorption has almost no effect at low frequencies, and only smoothes the transmission coefficient at higher frequencies, having little effect on the overall magnitude. It can be seen that the general behaviour of the calculated transmission coefficient and the positions of the lower and upper band edges agree well with the data. The first dip in the theoretical predictions is interesting, as it does not show up in the experimental data. It is also interesting that the transmission coefficient does not decrease monotonically towards the gap minimum and then rise monotonically throughout the rest of the gap, as in the case of the tungsten carbide/water crystals, but shows some structure. This structure shows up in both experiment and theory.

To examine the dependence of the transmission coefficient on sample thickness, a 7-layer tungsten carbide/epoxy sample was also constructed. The measured amplitude transmission coefficient, as well as the theoretical prediction from MST, is shown in Fig. 13. The data for the 4-layer sample are also included for comparison. First, it is obvious that the gap becomes deeper for the 7-layer sample, and that the decrease in amplitude at gap frequencies is approximately exponential, as expected for evanescent modes ($T \sim 10^{-4}$ and $\sim 10^{-7}$ for the 4-layer and 7-layer crystals, respectively). This large amplitude decrease near 2.5 MHz in the middle of the gap corresponds to an imaginary (evanescent) wave vector that is approximately 4 times larger than in the tungsten carbide/water crystals. As the thickness increases, the measured lower band edge shifts to higher frequency, from 1.22 MHz (for the 4-layer sample) to 1.37 MHz (for the 7-layer sample), while the position of the upper band edge almost remains the same for both samples. In the theoretical calculation, absorption in the epoxy matrix is included, as for the solid curve in Fig. 12. It can be seen that the general trends shown by the theory, as well as the positions of the lower and upper band edges, agree well with the data. The agreement is in fact excellent compared with previous transmission measurements and theory for 2D phononic crystals [34–35, 40–42], although it is not as good as that found for our water based crystals.

The band structure calculation shown in Fig. 3 predicts that the gap seen in these transmission experiments is a complete gap, covering the frequency range from about 1.5 MHz to 3.9 MHz. To investigate the existence of a complete gap experimentally, we measured the transmission along other crystal directions by rotating the crystal in the plane defined by Γ, K and L. The measurements were performed at 10 different angles, for angles α ranging up to 30° away from [111] towards the [110] direction, and for angles β up to 31.5° away from [111] towards the [001] direction. ($\alpha = 35.3°$ corresponds to the [110] or K direction, and $\beta = 54.7°$ corresponds to the [001] or X direction.) We found that the transmission coefficients in all these directions show a wide gap, and the positions of these gaps are close to the one along the [111] direction (corresponding to $\alpha = 0°$). For simplicity, we show only the results at the two largest angles, which are compared with the results measured along the [111] direction in Fig. 14. Despite the noise in the data at high frequencies, the gap properties can still be seen for all these crystal directions. In particular, the lower band edges for $\alpha = 30°$ and $\beta = 31.5°$ shift to lower frequencies compared with the [111] direction, which agrees well with the prediction of the band structure calculations, where the

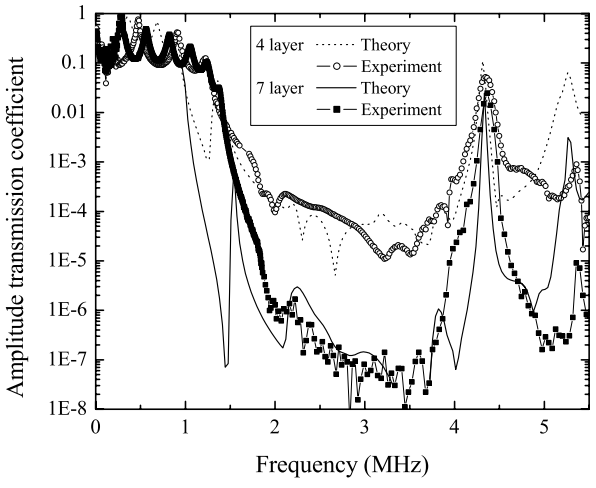

Fig. 13. Comparison of the amplitude transmission coefficients for 4-layer and 7-layer *fcc* phononic crystals made from tungsten carbide beads in epoxy.

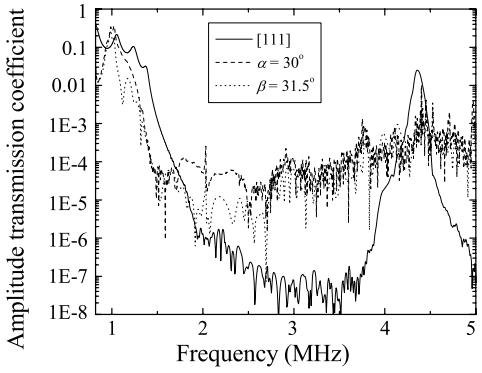

Fig. 14. Transmission coefficient measured for different angles of incidence relative to the [111] direction.

lower band edge is predicted to occur at lower frequencies along ΓK and ΓX than along ΓL. Thus, even though we have not attempted to correct these data for refraction at the crystal interfaces, the fact that the gap persists over such a wide range of angles supports the predictions of the band structure calculations that the band gap between 1.5 and 3.9 MHz is both wide and complete.

Given that the band gap in the tungsten carbide epoxy crystals is so large, one might expect that the group velocity would show even more extreme values in the vicinity of the band gap than were seen in the water-based crystals. Indeed for the 4-layer sample, the measured group velocity is around 15 mm/μs in the low frequency part of the band gap (near 1.7 MHz), about 4 times larger than for the tungsten carbide/water sample of the same thickness. Even larger values of the group velocity (reaching a maximum of 27 mm/μs) are predicted theoretically, even when the absorption in the epoxy is included in the MST calculations. However, the experimental data are fairly noisy due to the small signal levels. Thus, while the large values of the group velocity found between 1.5 and 2 MHz are consistent with a tunneling mechanism, we were not able to investigate the dependence of group time on crystal thickness in the current experiments, because signal to noise limitations precluded accurate measurements of v_g for the 7-layer crystal. Also, at higher frequencies within the gap, smaller values the group velocity are found, in both the experimental data and in theoretical calculations, raising interesting questions about the character of the modes seen in the gap at these higher frequencies. Further experiments are planned to investigate this behaviour in more detail. Another topic for future work is an in-depth study of the effects of absorption on the tunneling of ultrasound in the epoxy crystals, where the spatial distributions of both the absorption and the field are likely to be non-uniform.

6. Conclusions

Using pulsed ultrasound techniques and multiple-scattering theory (MST), we have systematically studied two types of phononic crystals – one with solid tungsten carbide beads immersed in water and another one with tungsten carbide (or steel) beads embedded in epoxy. Both crystal systems were found to exhibit complete band gaps. Besides investigating the band structures through both calculations and measurements, we also studied ultrasound tunneling and the anomalous dispersion of ultrasound near the band edges. Evidence for tunneling was shown by the increase in the group velocity with crystal thickness that is seen in both theory and experiment. In the absence of absorption, the ultrasound tunneling time was found to be independent of the phononic crystal thickness, with $t_{\text{tun}}\,\Delta\omega_{\text{gap}} \sim 1$ in the middle of the gap (here t_{tun} is the tunneling time and $\Delta\omega_{\text{gap}}$ is the width of the phononic band gap). Over the range of sample thicknesses that could be investigated experimentally, the tunneling time also appeared to approach a constant value; however the experimental tunneling time is larger than the theoretical predictions without absorption, an effect that is attributed to dissipation in the phononic crystals and is well explained by the two-modes model. By contrast, for very thick samples, our MST calculations show that the tunneling time no longer approaches a constant value but increases with thickness at a rate that is consistent with a constant, but large, group velocity. Thus in sufficiently thick crystals, the effect of absorption is to cause the weak propagating mode that results from incomplete destructive interference at gap frequencies to dominate, and obscure the dramatic effects of tunneling on pulse propagation.

In contrast to the very fast group velocities at gap frequencies that are seen in both experiment and theory, a strong suppression of the group velocity was found at the band edges, where large dispersive effects on pulse propagation were observed. This behaviour was characterized by measuring and calculating the group velocity dispersion (GVD), which plays a role in phononic crystals that is analogous to the reciprocal of the effective mass for electrons in semiconductors. Near the band edges, large oscillations in the GVD were found, while inside the band gap, the GVD was immeasurably small, indicating that ultrasound tunneling in phononic crytsals is essentially dispersionless.

The agreement between MST theory and the experiments is excellent in general. However, the differences between the experimental and theoretical results (mainly for the solid crystals) are compelling arguments for seeking possible future improvements to the theory, such as developing a first principles model for sound absorption in the crystals.

These fundamental studies of phononic crystals suggest a number of possible applications, which have also attracted considerable interest recently. One straightforward idea is based on the existence of complete gaps over certain frequency ranges. Since phononic properties scale well with frequency, one can change the position of the frequency gaps by simply altering the size of the building blocks. Thus phononic crystals are promising materials to shield noise for sophisticated devices over specific frequency ranges. Our solid tungsten carbide/epoxy crystal, which attenuates ultrasound very efficiently over a wide frequency range along all directions, can be a candidate for such application in ultrasonic devices. This type of phononic crystal could also be used as a sound mirror, as very little signal can penetrate the crystal at the gap frequencies, and most of the sound waves are strongly reflected back regardless the incident angle. Other applications based on the transmission properties are band pass filters, which have possible applications in transducer design.

More recently, attention has turned to another class of applications based on the focusing properties of phononic crystals, which exploit the negative refraction of ultrasound [49, 50]. The driving force behind much of this interest is the possibility of achieving better resolution than can be realized with conventional lenses, and the possibility of taking advantage of the novel beam bending capability of phononic crystals to shape narrow sound beams with good collimation. Such well-collimated sound beams could play an important role in future sound devices. These examples further illustrate the rich potential of phononic crystals in device applications that complement their importance for advancing our knowledge of wave transport in periodic media.

Acknowledgments. Support from NSERC of Canada, RGC (HKUST6143/00P) of Hong Kong, and NSFC (10174054) is gratefully acknowledged.

References

[1] Yablonovitch, E.: Inhibited Spontaneous Emission in Solid-State Physics and Electronics. Phys. Rev. Lett. **58** (1987) 2059–2062.
[2] John, S.: Strong localization of photons in certain disordered dielectric superlattices. Phys. Rev. Lett. **58** (1987) 2486–2489.
[3] Yablonovitch, E.; Gmitter, T. J.: Photonic band structure: The face-centered-cubic case. Phys. Rev. Lett. **63** (1989) 1950–1953.
[4] Leung, K. M.; Liu, Y. F.: Full vector wave calculation of photonic band structures in face-centered-cubic dielectric media. Phys. Rev. Lett. **65** (1990) 2646–2649.
[5] Zhang, Z.; Satpathy, S.: Electromagnetic wave propagation in periodic structures: Bloch wave solution of Maxwell's equations. Phys. Rev. Lett. **65** (1990) 2650–2653.
[6] Ho, K. M.; Chan, C. T.; Soukoulis, C. M.: Existence of a photonic gap in periodic dielectric structures. Phys. Rev. Lett. **65** (1990) 3152–3155.
[7] Soukoulis, C. M. (ed.): Photonic Band Gaps and Localization, Plenum Press, New York and London 1992.
[8] Joannopoulos, J. D.; Meade, R. D.; Winn, J. N.: Photonic crystals. Princeton University Press 1995.
[9] Mead, R. D.; Brommer, K. D.; Rappe, A. M.; Joannopoulos, J. D.: Electromagnetic Bloch waves at the surface of a photonic crystal. Phys. Rev. B**44** (1991) 10961–10964.
[10] Joannopoulos, J. D.; Villenneuve, P. R.; Fan, S.: Photonic crystals: putting a new twist on light. Nature (London) **386** (1997) 143–149.
[11] Lin, S.; Chow, E. C.; Hietala, V.; Villeneuve, P. R.; Joannopoulos, J. D.: Experimental Demonstration of Guiding and Bending of Electromagnetic Waves in a Photonic Crystal. Science **282** (1998) 274.
[12] Li, Z. Y.; Gu, B. Y.; Yang, G. Z.: Large Absolute Band Gap in 2D Anisotropic Photonic Crystals. Phys. Rev. Lett. **81** (1998) 2574–2577.
[13] Kosaka, H.; Kawashima, T.; Tomita, A.; Notomi, M.; Tamamura, T.; Sato, T.; Kawakami, S.: Superprism phenomena in photonic crystals. Phys. Rev. B**58** (1998) 10096–10099.
[14] Kosaka, H.; Kawashima, T.; Tomita, A.; Notomi, M.; Tamamura, T.; Sato, T.; Kawakami, S.: Self-collimating phenomena in photonic crystals. Appl. Phys. Lett. **74** (1999) 1212–1214. Kosaka, H.; Kawashima, T.; Tomita, A.; Notomi, M.; Tamamura, T.; Sato, T.; Kawakami, S.: Photonic crystals for micro lightwave circuits using wavelength-dependent angular beam steering. Appl. Phys. Lett. **74** (1999) 1370–1372.
[15] Foteinopoulou, S.; Economou, E. N.; Soukoulis, C. M.: Refraction in Media with a Negative Refractive Index. Phys. Rev. Lett. **90** (2003) 107402. Cubukcu, E.; Aydin, K.; Ozbay, E.; Foteinopoulou, S.; Soukoulis, C. M.: Electromagnetic waves: Negative refraction by photonic crystals. Nature **423** (2003) 604–605.
[16] John, S.: Electromagnetic Absorption in a Disordered Medium near a Photon Mobility Edge. Phys. Rev. Lett. **53** (1983) 2169–2172.
[17] John, S.: Localization of light. Phys. Today **44** No. 5 (May, 1991) 32–41.
[18] Soukoulis, C. M.; Economou, E. N.; Grest, G. D.; Cohen, M. H.: Existence of Anderson Localization of Classical Waves in a Random Two-Component Medium. Phys. Rev. Lett. **62** (1989) 575–578.
[19] Steinberg, A. M.; Kwiat, P. G.; Chiao, R. Y.: Measurement of the single-photon tunneling time. Phys. Rev. Lett. **71** (1993) 708–711.
[20] Spielmann, Ch.; Szipocs, R.; Stingl, A.; Krausz, F.: Tunneling of Optical Pulses through Photonic Band Gaps. Phys. Rev. Lett. **73** (1994) 2308–2311.
[21] Mojahedi, M.; Schamiloglu, E.; Hegeler F.; Malloy, K. J.: Time-domain detection of superluminal group velocity for single microwave pulses. Phys. Rev. E**62** (2000) 5758–5766.
[22] Imhof, A.; Vos, W. L.; Sprik, R.; Lagendijk, A.: Large Dispersive Effects near the Band Edges of Photonic Crystals. Phys. Rev. Lett. **83** (1999) 2942–2945.
[23] Sigalas, M.; Economou, E. N.: Band structure of elastic waves in two dimensional systems. Solid State Communications **86** (1993) 141–143. Economou, E. N.; Sigalas, M. M.: Classical wave propagation in periodic structures: Cermet versus network topology. Phys. Rev. B**48** (1993) 13434–13438. Economou, E. N.; Sigalas, M.: Stop bands for elastic waves in periodic composite materials J. Acoust. Soc. Am. **95** (1994) 1734–1740. Sigalas, M. M.; Economou, E. N.: Attenuation of multiple-scattered sound. Europhys. Lett. **36** (1996) 241–246. Kafesaki, M.; Sigalas, M. M.; Economou, E. N.: Elastic wave band gaps in 3-D periodic polymer matrix composites. Solid State Communications **96** (1996) 285–289.
[24] Kushwaha, M. S.; Halevi, P.; Dobrzynski, L.; Djafari-Rouhani, B.: Acoustic band structure of periodic elastic composites. Phys. Rev. Lett. **71** (1993) 2022–2025. Kushwaha, M. S.; Halevi, P.: Band-gap engineering in periodic elastic composites. Appl. Phys. Lett. **64** (1994) 1085–1087. Kushwaha, M. S.; Halevi, P.; Martínez, G.; Dobrzynski, L.; Djafari-Rouhani, B.: Theory of acoustic band structure of periodic elastic composites. Phys. Rev. B**49** (1994) 2313–2322. Kushwaha, M. S.; Djafari-Rouhani, B.: Complete acoustic stop bands for cubic arrays of spherical liquid balloons. J. Appl. Phys. **80** (1996) 3191–3195. Kushwaha, M. S.; Halevi, P.: Stop bands for cubic arrays of spherical balloons. J. Acoust. Soc. Am. **101** (1997) 619–622. Kushwaha, M. S.; Djafari-Rouhani, B.; Dobrzynski, L.; Vasseur, J. O.: Sonic stop-bands for cubic arrays of rigid inclusions in air. Eur. Phys. J. B**3** (1998) 155–161.
[25] Vasseur, J. O.; Djafari-Rouhani, B.; Dobrzynski L.; Deymier, P. A.: Acoustic band gaps in fibre composite materials of boron nitride structure. J. Phys.: Condens. Matter **9** (1997) 7327–7342.
[26] Kafesaki, M.; Economou, E. N.: Multiple-scattering theory for three-dimensional periodic acoustic composites. Phy. Rev. B**60** (1999) 11993–12001.
[27] Psarobas, I. E.; Stefanou, N.; Modinos, A.: Scattering of elastic waves by periodic arrays of spherical bodies. Phys. Rev. B**62** (2000) 278–291.
[28] Liu, Z.; Chan, C. T.; Sheng, P.; Goertzen, A. L.; Page, J. H.: Elastic wave scattering by periodic structures of spherical objects: Theory and experiment. Phys. Rev. B**62** (2000) 2446–2457.
[29] García-Pablos, D.; Sigalas, M.; Montero de Espinosa, F. R.; Torres, M.; Kafesaki M.; García, N.: Theory and Experiments on Elastic Band Gaps. Phys. Rev. Lett. **84** (2000) 4349–4352.
[30] Vasseur, J. O.; Deymier, P. A.; Chenni, B.; Djafari-Rouhani, B.; Dobrzynski, L.; Prevost, D.: Experimental and Theoretical Evidence for the Existence of Absolute Acoustic Band Gaps in Two-Dimensional Solid Phononic Crystals. Phys. Rev. Lett. **86** (2001) 3012–3015.
[31] Sigalas, M. M.: Elastic wave band gaps and defect states in two-dimensional composites. J. Acoust. Soc. Am. **101** (1997) 1256–1261. Sigalas, M. M.: Defect states of acoustic waves in a two-dimensional lattice of solid cylinders. J. Appl. Phys. **84** (1998) 3026–3030.
[32] Psarobas, I. E.; Stefanou, N.; Modinos, A.: Phononic crystals with planar defects. Phys. Rev. B**62** (2000) 5536–5540.
[33] Sprik, R.; Wegdam, G. H.: Acoustic band gaps in composites of solids and viscous liquids. Solid State Communications **106** (1998) 77–81.
[34] Mártinez-Sala, R.; Sancho, J.; Sánchez, J. V.; Linres, J.; Mesegure, F.: Sound attenuation by sculpture. Nature **378** (1995) 241.
[35] Montero de Espinosa, F. R.; Jimenez, E.; Torres, M.: Ultrasonic Band Gap in a Periodic Two-Dimensional Composite. Phys. Rev. Lett. **80** (1998) 1208–1211.
[36] Vasseur, J. O.; Deymier, P. A.; Frantziskonis, G.; Hong, G.; Djafari-Rouhani, B.; Dobrzynski, L.: Experimental evidence for the existence of absolute acoustic band gaps in two-dimensional periodic composite media. J. Phys.: Condens. Matter **10** (1998) 6051–6054.
[37] Sánchez-Pérez, J. V.; Caballero, D.; Mártinez-Sala, R.; Rubio, C.; Sánchez-Dehesa, J.; Meseguer, F.; Linares, J. ; Gálvez, F.: Sound Attenuation by a Two-Dimensional Array of Rigid Cylinders. Phys. Rev. Lett. **80** (1998) 5325–5328.

[38] Liu, Z.; Zhang, X.; Mao, Y.; Zhu, Y. Y.; Yang, Z.; Chan, C. T.; Sheng, P.: Locally Resonant Sonic Materials. Science **289** (2000) 1734–1736.

[39] Torres, M.; Montero de Espinosa, F. R.; Garcia-Pablos, D.; Garcia, N.: Sonic Band Gaps in Finite Elastic Media: Surface States and Localization Phenomena in Linear and Point Defects. Phy. Rev. Lett. **82** (1999) 3054–3057.

[40] Torres, M.; Montero de Espinosa, F. R.; Aragón, J. L.: Ultrasonic Wedges for Elastic Wave Bending and Splitting without Requiring a Full Band Gap. Phys. Rev. Lett. **86** (2001) 4282–4285.

[41] Page, J. H.; Goertzen, A. L.; Yang, S.; Liu, Z.; Chan, C. T.; Sheng, P.: Acoustic Band Gap Materials. In: *NATO ASI on Photonic Crystals and Light Localization* (Ed. C. M. Soukoulis) p. 59–68. Kluwer Academic Publishers 2001.

[42] Yang, S.; Page, J. H.; Liu, Z.; Cowan, M. L.; Chan, C. T.; Sheng, P.: Phononic crystals. Physics in Canada **57**(4) (2001) 187–189.

[43] Yang, S,; Page, J. H.; Liu, Z.; Cowan, M. L.; Chan, C. T.; Sheng, P.; Ultrasound tunneling through 3D phononic crystals. Phys. Rev. Lett. **88** (2002) 104301.

[44] Page, J. H.; Yang, Suxia; Cowan, M. L.; Liu, Zhengyou; Chan, C. T.; Sheng, Ping: 3D Phononic Crystals. In: *Wave Scattering in Complex Media: From Theory to Applications* (Eds. B. A. van Tiggelen, Sergey Skipetrov), p. 283–307. Kluwer Academic Publishers: NATO Science series, Amsterdam 2003.

[45] Sainidou, R.; Stefanou, N.; Modinos, A.: Formation of absolute frequency gaps in three-dimensional solid phoonic crystals. Phys. Rev. B**66** (2002) 212301.

[46] Cervera, F.; Sanchis, L.; Sanchez-Perez, J. V.; Martinez-Sala, R.; Rubio, C.; Meseguer, F.: Refractive Acoustic Devices for Airborne Sound. Phys. Rev. Lett. **88** (2002) 023902. Gupta, B. C.; Ye, Z.: Theoretical analysis of the focusing of acoustic waves by two-dimensional sonic crystals.. Phys. Rev. E**67** (2003) 036603.

[47] Garcia, N.; Nieto-Vesperinas, M.; Ponizovskaya, E. V.; Torres, M.: Theory for tailoring sonic devices: Diffraction dominates over refraction. Phys. Rev. E**67** (2003) 046606.

[48] Sainidou, R.; Stefanou, N.; Modinos, A.: Green's function formalism for phononic crystals. Phys. Rev. B**69** (2004) 064301.

[49] Yang, S.; Page, J. H.; Liu, Z.; Cowan, M. L.; Chan, C. T.; Sheng, P.: Focusing of Sound in a 3D Phononic Crystal. Phys. Rev. Lett. **93** (2004) 024301.

[50] Zhang, X.; Liu, Z.: Negative refraction of acoustic waves in two-dimensional phononic crystals. Appl. Phys. Lett. **85** (2004) 341–343.

[51] See also reference 45 for an examination of how the band gap width depends on the geometry of the structure.

[52] Hartman, T. E.: Tunneling of a wave packet. J. Appl. Phys. **33** (1962) 3427–3433.